ISSN 1062-7391, Journal of Mining Science, 2012, Vol. 48, No. 5, pp. 856–869. © Pleiades Publishing, Ltd., 2012.
Original Russian Text © N.I. Aleksandrova, 2012, published in Fiziko-Tekhnicheskie Problemy Razrabotki Poleznykh Iskopaemykh, 2012, No. 5, pp. 104–119.

ROCK FAILURE

Numerical-Analytical Investigation into Impact Pipe Driving in Soil with Dry Friction. Part I: Nondeformable External Medium

N. I. Aleksandrova

N.A. Chinakal Institute of Mining, Siberian Branch, Russian Academy of Sciences,
Krasnyi pr. 54, Novosibirsk, 630091 Russia
e-mail: alex@math.nsc.ru

Received August 20, 2012

Abstract—The study focuses on propagation of longitudinal waves in an elastic pipe partly embedded in a medium with dry friction. Mathematical formulation of the problem on the impact pipe driving into the soil is based on the model of longitudinal vibration of an elastic rod with taking into account lateral resistance. The lateral resistance of soil is described by the law of the contact dry friction. Numerical and analytical solutions to problems on longitudinal impulse loading of a pipe are compared.

Key words: Longitudinal waves, elastic rod, dry friction, impulse loading, numerical modeling.

INTRODUCTION

The problems of pipe "behavior" in soil arise in a variety of technological processes including impact driving and removal of piles, trenchless underground communication pipe laying by driving metallic pipes into soil, behavior of underground pipelines in earthquakes, or different rod elements in mechanical systems. The influence of friction between the soil and the side pipe surface on the wave process anyway remains a research issue of the prime importance. A good deal of R&D reports and transactions reviews the interaction of bodies with account for friction factor [1–21].

The problem of the longitudinal wave propagation in a rod when the rod's surface interacts with an ambient medium like a dry-friction model was studied in [3, 4, 6, 7, 11–21] by considering and analyzing the wave processes. In most publications the researchers defined the rod cross-section that segregates the disturbed section from the stationary section of the rod. A general method for solving these problems implies the reduction of the non-linear problem to a number of soluble consistently linear problems. The basic problem the researchers face is the identification of the range boundaries in time and in the longitudinal coordinate within which the magnitude and direction of the friction force remain constant. The friction force direction depends on the velocity sign in these waves. The solution in every range is performed with consideration for a preliminary determined sign of the velocity. The approach used in [3, 4, 6, 7, 11–18] made it possible to obtain the solution to a number of the problems under rather simple rod-loading laws.

In [3] the method of characteristics was helpful to study the problem of impacts on elastic rod partially embedded into a dry-friction medium. The problems of an impact at a constant velocity and a velocity monotonously increasing in time were solved. The researchers found the critical impact velocity at which the impact impulse front reaches the opposite end of the rod. In [4] the study subject is a moving rod of finite length with account for contact dry friction between the rod and ambient medium. Constant motion velocity is preset at the left end of the rod. Motion of the ambient medium is taken into account solely in the velocity of the moving lateral load applied. In this problem formulation, the analytical solutions are obtained by using the Laplace transformations. In [7] the research problem deals with the disturbance propagation within a rod at the side surface of which the dry-friction law is realized when one of rod's ends moves according to the harmonic law. The

approximated solutions were obtained using the methods of integrated amplitudes and the mechanical analogue. These two solutions coincide qualitatively and still differ quantitatively.

In [6, 11, 15] the researchers obtained analytical solution to the problem of exciting oscillations in a rod with the external dry friction and one rod end under the constant stress and the opposite rod end stiffly fixed. In [12–16] under consideration is the problem dealing with the dynamics of an elastic rod, one of its ends interacts with a mass striking it, and at the other end either a displacement or stress–displacement relation is preset pertaining to the character of the load applications. Besides, the gravity force of the rod and the stiff body, as well as the resistance under the law of the dry friction at the rod side surface, were taken into account. In [16] the solution to this problem is reported for an arbitrary time and the precise time of weight rebound from the rod.

In [17, 18] the studies cover the longitudinal oscillations of the elastic rod with a preset dry friction at the side surface and the stepwise loading of one of its ends with a period, being a multiple of a natural oscillation period for the system. The resonance excitation and the stabilized periodical oscillations of the system are analyzed.

Despite the great theoretical contribution gained in solving the problem the issues of the prime practical importance are left unsolved. For example, there are significant constraints on a character of the load applied to the rod, because under the smooth loading the front of the wave propagating along the rod moves slower as compared to a disturbance propagation velocity in the rod and it can be evaluated exclusively in solutions, but the latter is not always possible. Thereto, the most practical problems of the loading are complex.

Publications [19, 21] present the numerical solution. In [19] the solution to the problem of the wave propagation in a viscous –elastic rod with the external dry friction under a rectangular dynamic effect was obtained by the method of characteristics. In [21] the problem of the dynamic effect on a pipe with the Coulomb's dry friction was solved by the finite difference method.

Below the similar to [21] method for the end-to-end numerical calculation of the wave processes in the systems with dry friction permits to consider any load type because a direction and a magnitude of the friction force at every point and every time moment is preset in terms of the physical aspects in the course of a solving procedure. In this case the main problem is the testing of numerical algorithms and achievement of adequacy between discrete and continuum solutions. In view of this point the availability of analytical solutions is a compulsory condition. On the other hand, the analytical solutions in terms of some simplifying assumptions should be also verified on the correctness and the identification of the parameter domain of their validity.

In the present paper the research scientist obtained the approximated analytical solutions to the problem of the disturbance propagation in a rod of finite and infinite lengths with the external dry friction when a pulse stress is preset at one of its ends, while the other end is free of stresses.

1. STATEMENT OF THE PROBLEM

In the study problem an elastic tubular rod with radius *R,* wall thickness h, and length L is embedded in the soil at depth L_1. A longitudinal pulse $Q(t)$ is applied to its end. The constant shear stress τ_0 is applied in moving cross-sections at a side surface of the rod. The dry friction effect is accounted in the way similar to [13]. The origin of the selected coordinate system should coincide with the rod end, subjected to a percussion effect, axis z should be directed in parallel to the rod axis in-depth the medium. The rod motion is described by one-dimensional wave equation relative to displacements $U(t,z)$:

$$\ddot{U} = c^2 U''_{,zz} - k\tau, \quad \tau = \frac{\tau_0 P_t}{\rho S_t}, \quad k = \operatorname{sign}\dot{U}, \tag{1}$$

under zero initial conditions:

$$U\big|_{t=0} = 0, \quad \dot{U}\big|_{t=0} = 0 \tag{2}$$

and boundary conditions at the rod ends:

$$ES_t U'_{,z}\big|_{z=0} = -Q(t), \quad ES_t U'_{,z}\big|_{z=L} = 0. \tag{3}$$

In (1)–(3) $c = \sqrt{E/\rho}$ is a velocity of a longitudinal wave; ρ is density of a pipe material; E is Young modulus, $S_t = \pi h(2R - h)$ is area of the pipe cross-section, $P_t = 2\pi R$ is pipe perimeter.

2. SPECIFIC FEATURES OF NUMERICAL ALGORITHMS

The system of equations (1)–(3) was solved numerically for a single percussion. The finite difference scheme of "cross" type was used:

$$U_j^{n+1} - 2U_j^n + U_j^{n-1} = h_t^2\left[c^2(U_{j+1}^n - 2U_j^n + U_{j-1}^n)/h_z^2 - k\tau_j^n\right].$$

Here, $U_j^n = U(h_t n, h_z j)$ are displacements at time moments $t = h_t n$ at point coordinates $z = h_z j$, where h_t, h_z are steps of the computational mesh in coordinates t, z, $\tau_j^n = \tau(h_t n, h_z j)$. The optimal parameters of the difference net to provide the minimum numerical dispersion for a discrete analogue of equation (1) are $h_z = ch_t$ [22].

The calculation algorithm with account for the friction is: as neither direction nor friction force value are known the velocities of points for two possible signs are calculated at k ($k > 0$ and $k < 0$):

a) in the first case, introduce a fictive velocity $\dot{U}_j^+$:

$$\dot{U}_j^+ = \frac{U_j^+ - U_j^n}{h_t}, \quad U_j^+ = U_j^{n+1} - h_t^2\tau;$$

b) in the second case, introduce a fictive velocity $\dot{U}_j^-$:

$$\dot{U}_j^- = \frac{U_j^- - U_j^n}{h_t}, \quad U_j^- = U_j^{n+1} + h_t^2\tau.$$

In the above two cases, U_j^{n+1} is calculated from the finite difference analogue of equation (1) disregarding the friction.

Two situations can be observed:

1) at $\dot{U}_j^+$ and $\dot{U}_j^-$ of the same sign, the value U_j^k for which $|\dot{U}_j^k| = \min[|\dot{U}_j^-|, |\dot{U}_j^+|]$ is selected as the real values of displacements U_j^{n+1} from U_j^+ and U_j^-;

2) at $\dot{U}_j^+$ and $\dot{U}_j^-$ of different signs, or one of the velocities turned to zero, and under assumption of the passive friction, it is concluded that the real velocity of the pipe equals zero and, therefore, the friction force is absent. Values U_j^{n+1} are calculated at assumed $k = 0$.

Thus, the identification of boundaries of the motion area and other areas, being one of main hampering problems in the analytical solution, is reduced to finding points where $\dot{U}_j^+$ and $\dot{U}_j^-$ of different signs, or one of them, turn to zero. As a magnitude and a direction of the friction force are single-valued in calculations, every temporal layer implies solving a linear problem where the friction force is found and expressed as a load in the right side of the equation.

3. ANALYTICAL ESTIMATES

To test the finite difference algorithms, we obtain the approximated analytical estimates for a number of problems. Suggest that a semi-sinusoidal pulse load is applied to a section $z = 0$ of a semi-infinite rod with the acting dry contact friction at its side surface:

$$Q(t) = P_0 \sin(\omega_* t) H_0(t_0 - t) H_0(t), \quad \omega_* = \pi / t_0. \tag{4}$$

To obtain an analytical solution, we assume that the rod is infinite and the load is applied to cross-section $z = 0$ and perform the Laplace and Fourier transformations along t and z. The velocity in the infinite rod is positive, then $k = 1$ if $\dot{U} > 0$, and $k = 0$ if $\dot{U} = 0$. Note that the disturbance propagation velocity in a waveguide with account for the friction cannot exceed velocity c. In view of these two remarks, the solution in the images of the velocity of the pipe section displacements takes the form:

$$\dot{U}^{LF} = \frac{P_0 (1 + e^{-pt_0}) \omega_* p}{\rho S_t (\omega_*^2 + p^2)(p^2 + q^2 c^2)} - \frac{2\tau_0 P_t c p k}{\rho S_t (p^2 + q^2 c^2)^2}.$$

Inversion of the Laplace and Fourier transformations gives the following displacement velocity expression for an infinite rod:

$$\dot{U}(z,t) = \frac{1}{c\rho S_t} \left[\frac{P_0}{2} \sin \omega_* \left(t - \frac{|z|}{c} \right) H_0 \left(\frac{|z|}{c} - t + t_0 \right) - k \frac{\tau_0 P_t c t}{2} \right] H_0 \left(t - \frac{|z|}{c} \right).$$

In the case with a semi-infinite rod $(z \geq 0)$, we should provide the twofold increase in the pulse amplitude:

$$\dot{U}(z,t) = \frac{1}{c\rho S_t} \left[P_0 \sin \omega_* \left(t - \frac{z}{c} \right) H_0 \left(\frac{z}{c} - t + t_0 \right) - k \frac{\tau_0 P_t c t}{2} \right] H_0 \left(t - \frac{z}{c} \right).$$

Given that $\dot{U} > 0$, the function $k = 1$, so the result is an inequality for identification of a range at the plane (z, t) where $k = 1$:

$$\sin \omega_* \left(t - \frac{z}{c} \right) > \frac{\tau_0 P_t c t}{2 P_0}, \quad 0 \leq t - \frac{z}{c} \leq t_0.$$

For the given time moment t, we find the interval in z, where this inequality is fulfilled. Let z_1 satisfies the equation:

$$\sin \omega_* \left(t - \frac{z_1}{c} \right) = \frac{\tau_0 P_t c t}{2 P_0}.$$

Considering $\varepsilon = t - z_1 / c$, we obtain $k = 1$ within the interval $c(t - t_0 + \varepsilon) < z < c(t - \varepsilon)$. Beyond this interval, $\dot{U} = 0$ and $k = 0$. Therefore, we have the following approximated relation of the displacement velocity and coordinate z at fixed time t:

$$\dot{U}(z,t) = \frac{1}{c\rho S_t} \left[P_0 \sin \omega_* \left(t - \frac{z}{c} \right) - \frac{\tau_0 P_t c t}{2} \right] H_0 \left(\frac{z}{c} - t + t_0 - \varepsilon \right) H_0 \left(t - \frac{z}{c} - \varepsilon \right). \tag{5}$$

Here, ε is found from:

$$\sin(\omega_* \varepsilon) = \frac{\tau_0 P_t c t}{2 P_0} \tag{6}$$

and satisfies the inequality $0 \leq \varepsilon \leq t_0 / 2$.

It is revealed from the analysis of formula (5) that the maximum displacement velocity values are gained in the cross-section $z = c(t - t_0 / 2)$ and linearly depend on the pulse amplitude P_0 of shear stress τ_0 and time t:

$$\max \dot{U} = \frac{P_0}{c\rho S_t} - \frac{\tau_0 P_t t}{2\rho S_t} > 0.$$

It follows from this formula that in the semi-infinite rod with the applied external dry friction, the running pulse amplitude disappears at time moment:

$$t_* = \frac{2P_0}{\tau_0 P_t c}. \tag{7}$$

The estimate (7) coincides with the estimate obtained in [6].

As the disturbance propagation velocity in the rod equals to c, it follows from (7) that at:

$$z > z_* = c\left(t_* - \frac{t_0}{2}\right) = \frac{2P_0}{\tau_0 P_t} - \frac{ct_0}{2}, \tag{8}$$

no disturbances are present in the rod.

Let us fix coordinate z and establish the dependence of the displacement velocity on time. Let t_1, t_2 satisfy equations:

$$\sin\omega_*\left(t_1 - \frac{z}{c}\right) = \frac{\tau_0 P_t c t_1}{2P_0}, \quad \sin\omega_*\left(t_2 - \frac{z}{c}\right) = \frac{\tau_0 P_t c t_2}{2P_0}.$$

With account for symbols $\varepsilon_1 = t_1 - z/c$, $\varepsilon_2 = z/c + t_0 - t_2$, we obtain transcendental equations for evaluation of ε_1, ε_2:

$$\sin(\omega_*\varepsilon_1) = \frac{\tau_0 P_t c}{2P_0}\left(\varepsilon_1 + \frac{z}{c}\right), \quad \sin(\omega_*\varepsilon_2) = \frac{\tau_0 P_t c}{2P_0}\left(\frac{z}{c} + t_0 - \varepsilon_2\right),$$

where ε_1, ε_2 lie in the interval $0 \le \varepsilon_1 \le t_0/2$, $0 \le \varepsilon_2 \le t_0/2$. We obtain that $\dot{U} > 0$ and $k = 1$ in the domain $z/c + \varepsilon_1 < t < z/c + t_0 - \varepsilon_2$. Beyond this interval, $\dot{U} = 0$. Now, take the following relation of the displacement velocity on time at fixed coordinate z as an approximated solution:

$$\dot{U}(z,t) = \frac{1}{c\rho S_t}\left[P_0 \sin\omega_*\left(t - \frac{z}{c}\right) - \frac{\tau_0 P_t c t}{2}\right] H_0\left(\frac{z}{c} - t + t_0 - \varepsilon_2\right) H_0\left(t - \frac{z}{c} - \varepsilon_1\right). \tag{9}$$

Integrating (9), we obtain the dependence of the rod cross-section displacements on time and coordinate of the semi-sinusoidal pulse:

$$U(z,t) = \frac{1}{c\rho S_t}\begin{cases} \dfrac{P_0}{\omega_*}\left[\cos(\omega_*\varepsilon_1) + \cos(\omega_*\varepsilon_2)\right] - \dfrac{\tau_0 P_t c}{4}\left[\left(\dfrac{z}{c} + t_0 - \varepsilon_2\right)^2 - \left(\dfrac{z}{c} + \varepsilon_1\right)^2\right], & t - \dfrac{z}{c} > t_0 - \varepsilon_2, \\ \dfrac{P_0}{\omega_*}\left[\cos(\omega_*\varepsilon_1) - \cos\omega_*\left(t - \dfrac{z}{c}\right)\right] - \dfrac{\tau_0 P_t c}{4}\left[t^2 - \left(\dfrac{z}{c} + \varepsilon_1\right)^2\right], & \varepsilon_1 \le t - \dfrac{z}{c} \le t_0 - \varepsilon_2, \\ 0, & t - \dfrac{z}{c} < \varepsilon_1. \end{cases} \tag{10}$$

Given that an arbitrary pulse effect is preset in the interval $(0, t_0)$:

$$Q(t) = P_0\widetilde{Q}(t)H_0(t_0 - t)H_0(t),$$

where $\widetilde{Q}(t)$ is a convex function, we follow the analogous procedure and obtain an approximated dependence of the displacement velocity on the time t at the fixed coordinate z:

$$\dot{U}(z,t) = \frac{1}{c\rho S_t}\left[P_0\widetilde{Q}\left(t - \frac{z}{c}\right) - \frac{\tau_0 P_t c t}{2}\right] H_0\left(\frac{z}{c} - t + t_0 - \varepsilon_2\right) H_0\left(t - \frac{z}{c} - \varepsilon_1\right), \tag{11}$$

$$2P_0\widetilde{Q}(\varepsilon_1) = \tau_0 P_t(z + c\varepsilon_1), \quad 2P_0\widetilde{Q}(t_0 - \varepsilon_2) = \tau_0 P_t(z + ct_0 - c\varepsilon_2).$$

In the case of a rectangular-shaped pulse, $\varepsilon_1 = \varepsilon_2 = 0$ and the displacements resulted from the integration of (11), no doubt, satisfy equation (1). For different-shaped pulses, (1) in solution (11) is satisfied approximately but with higher precision when the term $t_0 << t_*$ is fulfilled.

Note that (5), (10), (11) are derived under assumption that $k = 1$ if $\dot{U} > 0$ and $k = 0$ if $\dot{U} = 0$. This term is fulfilled within the entire interval of the disturbance propagation under the correct-shaped pulse, given that $t_0 \le t_*$. If $t_0 > t_*$, displacement velocity can assume negative value at a certain time moment under assumption that $k = -1$. In this case, the solution is different.

Consider a rod of a finite length L with dry friction, shear stress τ_0, and semi-sinusoidal longitudinal load all applied to its side surface (4). It follows from (9), in a rod with $L > z_*$ the end being opposite to the point of the force application does not "feel" this effect. It is possible to find from (9) the required pulse amplitude to enable the disturbance to reach the pipe end:

$$P_0 \ge \left(L + \frac{ct_0}{2} \right) \frac{\tau_0 P_t}{2}.$$

If $L >> ct_0 / 2$, the second term can be neglected and the result is:

$$P_0 \ge F_{\text{fr}} / 2, \quad F_{\text{fr}} = \tau_0 P_t L, \tag{12}$$

i.e., the pulse amplitude should at least a half higher than the friction force F_{fr} acting at the side surface of the pipe.

Taking into account the rebounds from the rod ends, the approximated solution to the study problem for displacement velocities is: русские индексы! (все формулы ниже проверить)

$$\begin{aligned} \dot{U}(z,t) = &\sum_{n=0}^{n_1} \frac{1}{c\rho S_t} \left\{ P_0 \sin \omega_* (t - a_{2n} + \varepsilon_{11n}) - F_{\text{fr}} \frac{ct}{2L} \right\} H_0(t - a_{2n}) H_0(a_{1n} - t) + \\ &+ \sum_{n=0}^{n_2} \frac{1}{c\rho S_t} \left\{ P_0 \sin \omega_* (t - b_{2n} + \varepsilon_{21n}) - F_{\text{fr}} \frac{ct}{2L} \right\} H_0(t - b_{2n}) H_0(b_{1n} - t), \\ n_1 = &\left[\frac{P_0}{F_{\text{тр}}} - \frac{z}{2L} \right], \quad n_2 = \left[\frac{P_0}{F_{\text{fr}}} + \frac{z}{2L} - 1 \right], \end{aligned} \tag{13}$$

$$\sin(\omega_* \varepsilon_{11n}) = \frac{F_{\text{fr}}}{P_0} \left(n + \frac{z + c\varepsilon_{11n}}{2L} \right), \quad \sin(\omega_* \varepsilon_{12n}) = \frac{F_{\text{fr}}}{P_0} \left(n + \frac{z + c(t_0 - \varepsilon_{12n})}{2L} \right),$$

$$\sin(\omega_* \varepsilon_{21n}) = \frac{F_{\text{fr}}}{P_0} \left(n + 1 - \frac{z - c\varepsilon_{21n}}{2L} \right), \quad \sin(\omega_* \varepsilon_{22n}) = \frac{F_{\text{fr}}}{P_0} \left(n + 1 - \frac{z - c(t_0 - \varepsilon_{22n})}{2L} \right),$$

$$a_{1n} = \frac{2Ln + z}{c} + t_0 - \varepsilon_{12n}, \quad a_{2n} = \frac{2Ln + z}{c} + \varepsilon_{11n},$$

$$b_{1n} = \frac{2L(n+1) - z}{c} + t_0 - \varepsilon_{22n}, \quad b_{2n} = \frac{2L(n+1) - z}{c} + \varepsilon_{21n}.$$

The square brackets in (13) denote an integral part of a number. Integration of (13) in time gives the relation of the rod cross-section displacements vs. time and a longitudinal coordinate:

$$U(z,t) = \sum_{n=0}^{n_1} U_{1n} + \sum_{n=0}^{n_2} U_{2n}, \tag{14}$$

$$U_{1n}(z,t)=\frac{1}{c\rho S_t}\begin{cases}\dfrac{P_0}{\omega_*}\left[\cos(\omega_*\varepsilon_{11n})+\cos(\omega_*\varepsilon_{12n})\right]-\dfrac{\tau_0 P_t c}{4}(a_{1n}^2-a_{2n}^2), & t>a_{1n},\\ \dfrac{P_0\left[\cos(\omega_*\varepsilon_{12n})-\cos\omega_*(t-a_{2n}+\varepsilon_{11n})\right]}{\omega_*}-\dfrac{\tau_0 P_t c}{4}(t^2-a_{2n}^2), & a_{2n}\le t\le a_{1n},\\ 0, & t<a_{2n},\end{cases}$$

$$U_{2n}(z,t)=\frac{1}{c\rho S_t}\begin{cases}\dfrac{P_0}{\omega_*}\left[\cos(\omega_*\varepsilon_{21n})+\cos(\omega_*\varepsilon_{22n})\right]-\dfrac{\tau_0 P_t c}{4}(b_{1n}^2-b_{2n}^2), & t>b_{1n},\\ \dfrac{P_0}{\omega_*}\left[\cos(\omega_*\varepsilon_{22n})-\cos\omega_*(t-b_{2n}+\varepsilon_{21n})\right]-\dfrac{\tau_0 P_t c}{4}(t^2-b_{2n}^2), & b_{2n}\le t\le b_{1n}.\\ 0, & t<b_{2n}.\end{cases}$$

Evaluate a cumulative slip of a pipe in the cross-section $z=0$ at a time moment $t>b_{1n_*}$, namely, after the disturbances in the pipe are decayed under action of friction. It follows from (14):

$$U_1^*=\frac{1}{c\rho S_t}\sum_{n=0}^{n_*}\left(\frac{P_0}{\omega_*}\left[\cos(\omega_*\varepsilon_{11n})+\cos(\omega_*\varepsilon_{12n})\right]-\frac{F_{\text{fr}}c}{4L}(t_0-\varepsilon_{11n}-\varepsilon_{12n})\left(t_0+\frac{4Ln}{c}+\varepsilon_{11n}-\varepsilon_{12n}\right)\right)$$
$$+\frac{1}{c\rho S_t}\sum_{n=0}^{n_*-1}\left(\frac{P_0}{\omega_*}\left[\cos(\omega_*\varepsilon_{21n})+\cos(\omega_*\varepsilon_{22n})\right]-\frac{F_{\text{fr}}c}{4L}(t_0-\varepsilon_{21n}-\varepsilon_{22n})\left(t_0+\frac{4L(n+1)}{c}+\varepsilon_{21n}-\varepsilon_{22n}\right)\right),\quad(15)$$

$$n_*=\left[\frac{P_0}{F_{\text{fr}}}\right],\quad \sin(\omega_*\varepsilon_{11n})=\frac{F_{\text{fr}}}{P_0}\left(n+\frac{c\varepsilon_{11n}}{2L}\right),\quad \sin(\omega_*\varepsilon_{12n})=\frac{F_{\text{fr}}}{P_0}\left(n+\frac{c(t_0-\varepsilon_{12n})}{2L}\right),$$
$$\sin(\omega_*\varepsilon_{21n})=\frac{F_{\text{fr}}}{P_0}\left(n+1+\frac{c\varepsilon_{21n}}{2L}\right),\quad \sin(\omega_*\varepsilon_{22n})=\frac{F_{\text{fr}}}{P_0}\left(n+1+\frac{c(t_0-\varepsilon_{22n})}{2L}\right).$$

Assume that n_* is high enough, and approximated sum can be found by integration instead of the summing. We obtain rough estimate of the cumulative slip of the pipe as a result of multiple reflections of a semi-sinusoidal pulse:

$$U_1^*=\frac{t_0}{2c\rho S_t F_{\text{fr}}}\left\{P_0^2+2P_0F_{\text{fr}}\left(1+\frac{2}{\pi}\left(1+\frac{t_0c}{2L}\right)\right)-F_{\text{fr}}^2\frac{t_0c}{2L}\right\}.\quad(16)$$

From the formula, if the impact energy equals $t_0P_0^2/2$, the cumulative slip is proportional to "impact energy with account for friction" $t_0\widetilde{P}_0^2/2$, where:

$$\widetilde{P}_0^2=\left\{P_0^2+2P_0F_{\text{fr}}\left(1+\frac{2}{\pi}\left(1+\frac{t_0c}{2L}\right)\right)-F_{\text{fr}}^2\frac{t_0c}{2L}\right\}$$

and inversely proportional to the friction force.

The analogue formula for a rectangular pulse is:

$$Q(t)=P_0H_0(t)H_0(t_0-t).\quad(17)$$

It follows from (11) that the dependence of the velocity on time and loading coordinate (17) is:

$$\dot{U}(z,t)=\sum_{n=0}^{n_1}\frac{1}{c\rho S_t}\left\{P_0-F_{\text{fr}}\frac{ct}{2L}\right\}H_0(t-a_{2n})H_0(a_{1n}-t)+\quad(18)$$

$$+\sum_{n=0}^{n_2}\frac{1}{c\rho S_t}\left\{P_0 - F_{\text{fr}}\frac{ct}{2L}\right\}H_0(t-b_{2n})H_0(b_{1n}-t),$$

where $n_1 = \left[\frac{P_0}{F_{\text{fr}}} - \frac{z}{2L}\right]$, $n_2 = \left[\frac{P_0}{F_{\text{fr}}} + \frac{z}{2L} - 1\right]$, $a_{1n} = \frac{2Ln+z}{c} + t_0$, $a_{2n} = \frac{2Ln+z}{c}$, $b_{1n} = \frac{2L(n+1)-z}{c} + t_0$, $b_{2n} = \frac{2L(n+1)-z}{c}$.

Integration of (18) in time and assumption that $z = 0$ and $t > b_{1n_*}$ give the following value for the cross-section displacement $z = 0$ after all the disturbances decayed in the pipe:

$$U_2^* = \frac{t_0}{c\rho S_t}\sum_{n=0}^{n_*}\left(P_0 - \frac{F_{\text{fr}}c}{4L}\left(t_0 + \frac{4Ln}{c}\right)\right) + \frac{t_0}{c\rho S_t}\sum_{n=0}^{n_*-1}\left(P_0 - \frac{F_{\text{fr}}c}{4L}\left(t_0 + \frac{4L(n+1)}{c}\right)\right), \quad n_* = \left[\frac{P_0}{F_{\text{fr}}}\right],$$

$n_* = \left[\frac{P_0}{F_{\text{fr}}}\right]$.

In this case all the sums are computed explicitly with the result:

$$U_2^* = \frac{t_0}{2c\rho S_t}\left\{\left(P_0 - F_{\text{fr}}\frac{t_0 c}{4L}\right)\left(1 + 2\left[\frac{P_0}{F_{\text{fr}}}\right]\right) - F_{\text{fr}}\left(\left[\frac{P_0}{F_{\text{fr}}}\right] + 1\right)\left[\frac{P_0}{F_{\text{fr}}}\right]\right\}. \tag{19}$$

Given that $P_0 >> F_{\text{fr}}$, (19) can be rewritten as:

$$U_2^* \approx \frac{t_0}{2c\rho S_t F_{\text{fr}}}\left\{\left(P_0 - F_{\text{fr}}\frac{t_0 c}{4L}\right)^2 - F_{\text{fr}}^2\frac{t_0 c}{4L}\right\}. \tag{20}$$

This formula is similar to (16).

4. COMPARISON OF NUMERICAL CALCULATION DATA WITH ANALYTICAL ESTIMATES

Figures 1 and 2 demonstrate the curves of the displacement velocity in a pipe completely embedded in soil and the longitudinal coordinate under a semi-sinusoidal pulse without reflections $L_1 = L = 100$ m in Fig. 1 and with reflections $L_1 = L = 30$ m in Fig. 2 at different time moments. The vertical dash-and-dot line corresponds to the pipe cross-section $z = z_*$. The parameters of the problem are: $P_0 = 989.6$ kN; $t_0 = 0.25$ ms; $E = 203$ GPa; $h = 0.01$ m; $R = 0.1625$ m; $\rho = 7805$ kg/m^3; $h_z = 0.1$ m; $\tau_0 = 0.02$ MPa.

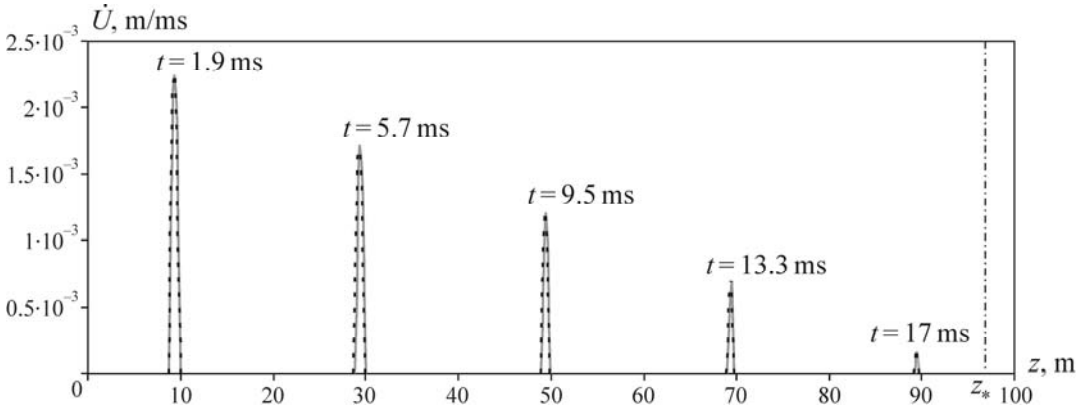

Fig. 1. Curves of displacement velocities at different time moments. Continuous curves—numerical experimental results, dotted curves—analytical solution (5).

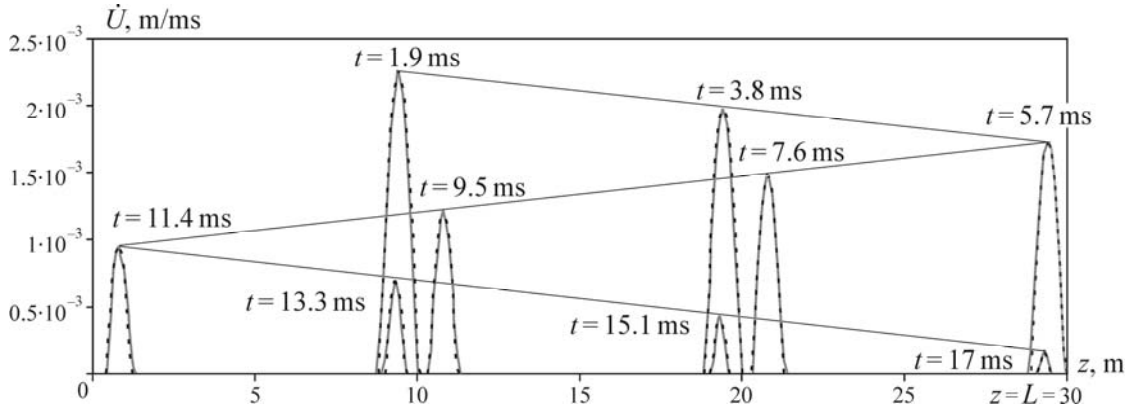

Fig. 2. Curves of displacement velocities at different time moments with account for reflection from rod ends at $L = 30$ m. Continuous curves—numerical experimental results, dotted curves—analytical solutions (5) and (13).

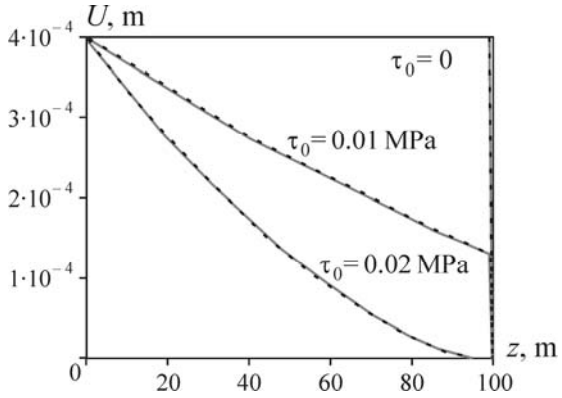

Fig. 3. Curves of displacements in pipe 100 m in length at time moment $t = 19.6$ ms and different τ_0 values: continuous curves—numerical experimental results, dotted curves—analytical solution (10).

From the comparison of the graphs, it is obvious that the numerical and analytical solutions coincide with high accuracy. It is worth noting that $t_0 / t_* = 0.013 << 1$ for the given parameters. Estimates (8) and (9) give the following values: the decaying time $t_* = 19.6$ ms for the longitudinal pulse and $z < z_* = 96.9$ m in the rod section occupied by disturbances, the cited data are confirmed by the numerical calculation results in Figs. 1 and 2. The analysis of the numerical and analytical solutions in Figs. 1 and 2 reveals that the friction effect leads to the situation when a lower portion of a pulse is progressively "faded" until the pulse decays completely.

In Fig. 3 the displacement curves are plotted for a pipe 100 m in length at time moment $t = 19.6$ ms and different τ_0 values. The other parameters remain the same as in Figs. 1 and 2. The analytical and numerical solutions coincide with high accuracy as well.

In Figs. 4 and 5, the oscillograms present the numerical and analytical solutions to displacements and displacement velocities of the pipe section $z = 0$ under the semi-sinusoidal effect. The parameters of the problem are: $P_0 = 88$ kN, $t_0 = 0.22$ ms, $L = L_1 = 4$ m, $E = 210$ GPa, $h = 0.003$ m, $R = 0.045$ m, $\rho = 7530$ kg/m^3, $h_z = 0.1$ m, $\tau_0 = 0.003$ MPa. The vertical dash-and-dot lines indicate the reflected waves at time moments $t = 2L/s$ and $t = 4L/s$. The continuous line is the numerical solution and the dotted line is the analytical solution where reflection is only taken into account.

The comparison of the numerical calculation results at different values of parameters in formulae (5), (10), (13), and (14) shows that the numerical and approximated analytical solutions coincide with high accuracy under condition that $t_0 << t_*$.

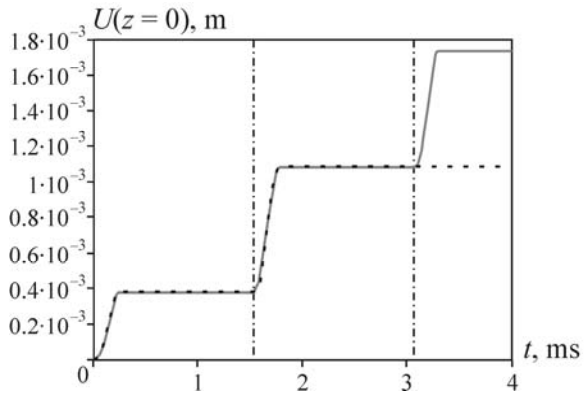

Fig. 4. Oscillograms of displacements in cross-section $z = 0$.

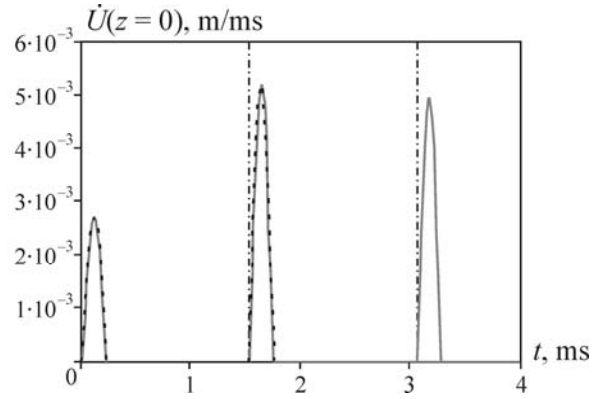

Fig. 5. Oscillograms of displacement velocities in cross-section $z = 0$.

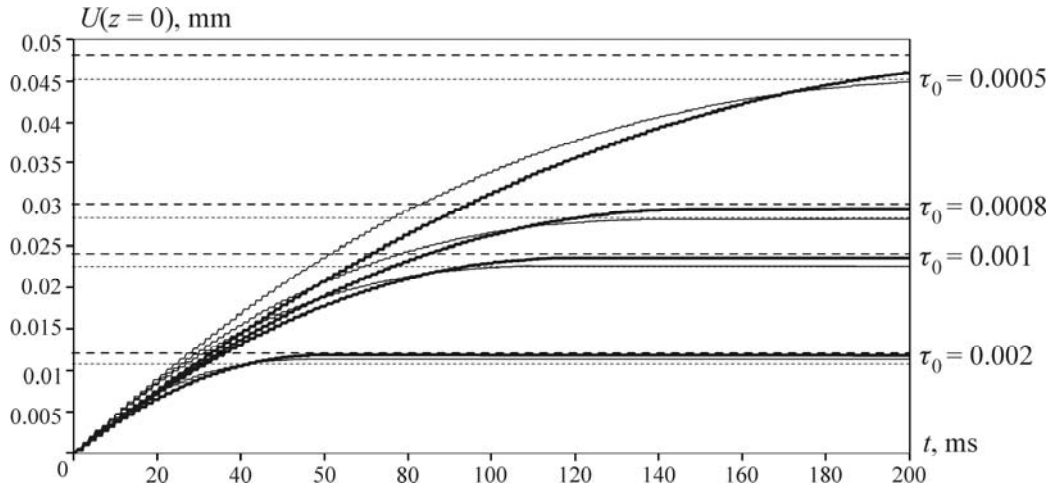

Fig. 6. Oscillograms of displacements of pipe section $z = 0$: thin lines—solution for effect (4) and thick lines—for pulse (17).

Thus, the pipe slip is rather closely and qualitatively correctly evaluated by rough estimates (16) and (19) for different-shaped pulses, but with the same impact energy amounting to $P_0^2 t_0 / 2$ in the given case, and the same friction force.

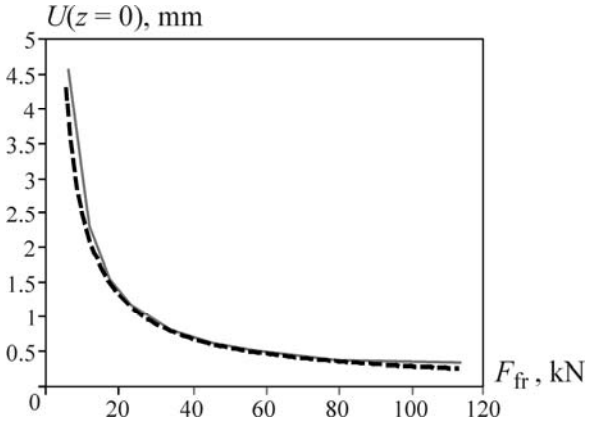

Fig. 7. Relationship between the displacements and friction force F_{f} at time moment $t = 100$ ms under the semi-sinusoidal pulse action.

Figure 7 presents the curves of displacements at time moment $t = 100$ ms under friction F_{fr} and semi-sinusoidal pulse. The curves are calculated by the finite difference method for a pipe partially embedded in soil at the following parameters: $L = 7.5$ m, $L_1 = 4$ m, $P_0 = 88$ kN, $t_0 = 0.22$ ms, $h = 0.003$ m, $R = 0.045$ m, $\rho = 7530$ kg/m^3, $E = 210$ GPa, $h_z = 0.1$ m. The solid curve is the finite difference solution, the dashed curve is the approximation of the finite difference solution: $F(F_{fr}) = 21.961 F_{fr}^{-0.9413}$, being very close to the function $21.961 / F_{fr}$. Given that $F_{fr} \le 2P_0$, the pipe is slipping relative to the medium. The qualitative behavior of the dependence of the pipe displacement per single impact under the friction effect coincides with the experimental results reported in [23] for the end and cone connection of an adapter and a pipe.

In Figs. 8 and 9, the numerical results are shown for the displacements of pipe section $z = 0$ at different pipe length values: $L = 3.5$ m $+ L_1$, the other parameters are identical to those in Fig. 7.

Figure 8 demonstrates ocsillograms of displacements. In Fig. 9 the solid line is the dependence of displacements at time moment $t = 100$ ms on the length L_1 of the pipe section embedded in soil. The dashed line corresponds to the approximation of the numerical experimental results for $F(L_1) = 4.28 L_1^{-0.9448}$. This function is very close to the function $4.28 / L_1$. Thus, for the partially-embedded pipe, the qualitative dependence on L_1 coincides with that obtained from formula (16) for the pipe completely embedded in soil.

The dependences of the maximums of velocity on distance obtained numerically at the parameters: $L = L_1 = 100$ m, $E = 203$ GPa, $h = 0.01$ m, $R = 0.1625$ m, $\rho = 7805$ kg/m^3, $h_z = 0.1$ m, $\tau_0 = 0.02$ MPa, which are identical to those in [24] for the other model, are plotted in Fig. 10: curve *1* corresponds to $\sigma_0 = 50$ MPa, $t_0 = 1$ ms; curve *2*—$\sigma_0 = 70.7$ MPa, $t_0 = 0.5$ ms; curve *3*—$\sigma_0 = 100$ MPa, $t_0 = 0.25$ ms at $\sigma_0 = P_0 / S_t$. Curves *1–3* and [24] coincide qualitatively and quantitatively and are described with high accuracy by Eqs. (5).

Figure 11 presents distribution of the displacements along the pipe at time moment 19.6 ms for different amplitudes and durations of semi-sinusoidal pulses, selected in such a way that their impact energy coincides and amounts to $P_0^2 t_0 / 2$. The solid line is analytical solution (10), the dash-and-dot line is the numerical calculations with the parameters identical to those in Fig. 10. It is evident that the analytical solution describes the numerical solution with high precision except for the close-to-impact area. These curves qualitatively and quantitatively coincide with the calculations in the model in [24].

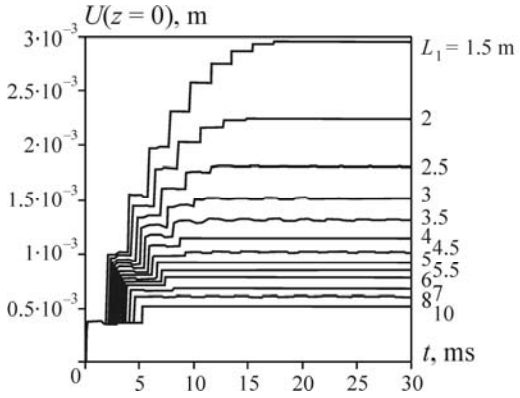

Fig. 8. Oscillograms of displacements at different length of the pipe embedded in soil.

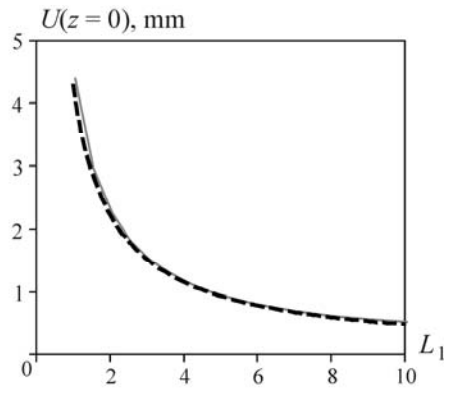

Fig. 9. Dependence of displacements on length of the pipe embedded in soil at $t = 100$ ms.

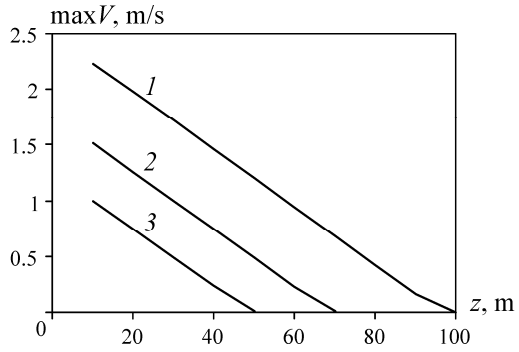

Fig. 10. Velocity maximums versus distance (described in the text).

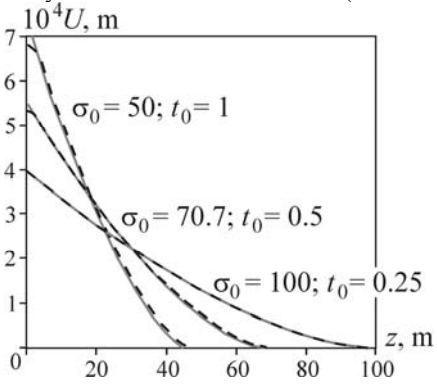

Fig. 11. Displacements at time moment 19.6 ms.

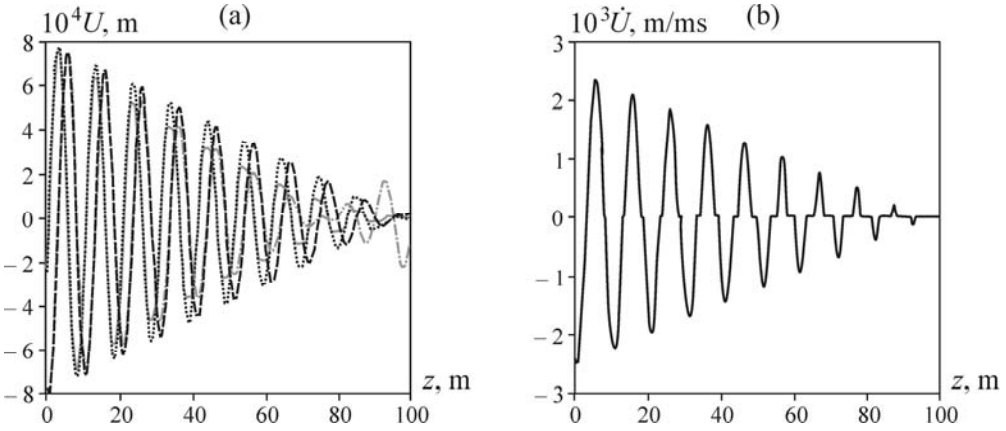

Fig. 12. Displacement curves: (a) solid curve—finite difference solution; dashed curve—solution (22); dash-and-dot curve—solution (21); dotted curve—solution (23); (b) displacement velocity curves.

In Fig. 12 the results are calculated at time moment 19.6 ms under the sinusoidal load applied to a rod end:

$$ES_t \frac{\partial u}{\partial x} = -P_0 \sin(\omega_* t) H_0(t) .$$

The parameters of the problem are: $\omega_* = 3.14$ ms^{-1}, $\sigma_0 = 100$ MPa, $t_0 = 1$ ms, the other parameters are identical to those in Fig. 10.

In Fig. 12a the displacement curves are presented. The solid line corresponds to the finite difference solution of (1)–(3), the dashed-and-dot line is the approximated analytical solution obtained by the method of the mechanical analogue [7]:

$$U(z,t) = \left(A_0 - \frac{2\tau_0 P_t z}{\pi c \omega_* \rho S_t} \right) \sin\left(\omega_* t - \frac{\omega_* z}{c} \right), \quad A_0 = \frac{2c}{\pi \omega_*} \sqrt{\left(\frac{\pi P_0}{2ES_t} \right)^2 - \left(\frac{\tau_0 P_t}{c \omega_* \rho S_t} \right)^2} . \qquad (21)$$

The dashed line is the approximated analytical solution obtained by the method of complex amplitudes [7]:

$$U(z,t)=\left(A_0-\frac{\tau_0 P_t z}{2c\omega_* \rho S_t}\right)\sin\left(\omega_* t-\frac{\omega_* z}{c}\right). \tag{22}$$

In Fig. 12b the graphs of the displacement velocity are presented. The comparison of the cited results makes it possible to conclude that the solution obtained by the method of the mechanical analogue, (21), gives high error in the area of the running disturbance front, but with increase in the distance from the front, the method gives the correct amplitude of oscillations. The solution obtained by the method of complex amplitudes, (22,) gives less error nearby the front, but beyond the front the oscillation amplitude is appreciably higher as compared to that calculated in the finite difference solution. The oscillation phase does not coincide with the numerical solution of equations (1)–(3) in both analytical solutions [7]. It is explicit that as the stresses at the rod end are preset by the sinusoidal function, the displacements after integration should be evaluated through cosines. The second summand in expression (21) for A_0 amounts to less than 0.05% of the first summand at the cited parameters, so it can be neglected. As it was mentioned above, the disturbances in the rod with dry friction at its side surface are absent in domain $z > z_*$. Taking into account these three remarks, we rewrite formula (22) as:

$$U(z,t)=\frac{P_0+\tau_0 P_t/2}{\omega_* \rho c S_t}\cos\left(\omega_* t-\frac{\omega_* z}{c}\right)H_0(z_*-z). \tag{23}$$

In Fig. 12a the dashed curve corresponds to expression (23). As it follows from three solutions (21)–(23), solution (23) is the closest to the finite difference solution. It is seen in the velocity curves how the reduction in every half-oscillation proceeds in case of harmonic disturbances. Given that the sinusoidal effect is assumed as a sum of semi-sinusoids and considering the velocity sign for every of these semi-sinusoids, it is possible to obtain more precise solution expressed as the sum of a series from formulae (5) and (10) as compared to solution (23). We do not present this solution because of its bulkiness. The finite difference solution was also compared to the well known analytical one [13], the obtained results were merging in the plots.

CONCLUSION

The finite difference algorithm for calculation of the wave processes in a pipe driven into soil is developed with account for the external dry friction. The approximated analytical solutions to the longitudinally one-dimensional problem for a pipe under external dry friction and an arbitrary-shaped longitudinal pulse have been obtained for both a semi-infinite pipe and a finite-length pipe with account for the pulse reflections from its end. The comparison of the finite difference and analytical solutions revealed their good compliance.

The finite difference calculations of the disturbances in a pipe under pulse effect with account for the contact dry friction at its side surface were made for wide ranges of the parameters of the problem. It is established that in the case with the finite-length pipe, the pipe displacements within a large time interval, as compared to the period of to-and-fro wave run along the pipe at the velocity of longitudinal waves, is proportional to “an impact energy with account for friction” and the pulse duration and reverse proportional to the friction force.

ACKNOWLEDGMENTS

The author is grateful to Dr. Eng. E.N. Sher and PhD Eng. V.A. Saraikin for their contribution to the present paper.

REFERENCES

1. Kragel'sky, I.V. and Shchedrov, V.S., *Razvitie nauki o trenii. Sukhoe trenie* (Advance in the Friction Science. Dry Friction), Moscow: Izd. AN SSSR, 1956.
2. Mikhin, N.M., *Vneshnee trenie tverdykh tel* (External Friction of Solids), Moscow: Nauka, 1977.
3. Veklich, N.A. and Malyshev, B.M., Wave Propagation in Elastic Rods Embedded in a Medium with Dry Friction, *Zadachi mekhaniki tverdogo tela* (Problems of Solid Body Mechanics), Moscow: MGU, 1985.
4. Ormonbekov, T., *Mekhanika vzaimodeistviya deformiryemykh tel* (Mechanics of Interaction of Deformable Bodies), Frunze: ILIM, 1989.
5. Markeev, A.P., *Dinamika tela, soprikasayushchegosya s tverdoi poverkhnost'yu* (Dynamics of a Body in Contact with Solid Surface), Moscow: Nauka, 1992.
6. Nikitin L. V., *Statika i dinamika tverdykh tel s sukhim treniem* (Statics and Dynamics of Solid Bodies with Dry Friction), Moscow: Moskovskii litsei, 1998.
7. Yunin, E.K., *Zagadki i paradoksy sukhogo treniya* (Dry Friction: Whys and Paradoxes), Moscow: LIBROKOM, 2008.
8. Rozenblat, G.M., *Sukhoe trenie i odnostoronnie svyazi v mekhanike tverdogo tela* (Dry Friction and Unilateral Bonds in Solid Body Mechanics), Moscow: URSS, 2010.
9. Andronov, V.V. and Zhuravlev, V.F., *Sukhoe trenie v zadachakh mekhaniki* (Dry Friction in Mechanics Problems), Moscow-Izhevsk: Regulyarnaya i khaoticheskaya dinamika, 2010.
10. Ivanov, A.P., *Osnovy teorii system s sukhim treniem* (Fundamentals of the Theory of the Dry Friction Systems), Moscow-Izhevsk: Regulyarnaya i khaoticheskaya dinamika, 2011.
11. Nikitin, L.V. and Tyurekhodgaev, A.N., The Dry Friction Damping of Dynamic Loads in Fiber Composite Materials, *Mekh. Kompozit. Mater*., 1986, no. 1.
12. Nikitin, L.V. and Tyurekhodgaev, A.N., Behavior of a Loaded Elastic Rod Embedded in Soil, *Problemy mekhaniki gornykh porod* (Problems of Rock Mechanics), Alma-Ata: Nauka, 1966.
13. Nikitin, L.V., Solid Body Impact on Elastic Rod with External Dry Friction, *Inzh. Zh. MTT*, 1967, no. 2.
14. Nikitin, L. V., Dynamics of Elastic Rods with External Dry Friction, *Usp. Mekh*., 1988, vol. 11, issue 4.
15. Zharkova, N.V. and Nikitin, L.V., Applied Problems of Elastic Rod Dynamics, *Izv. RAN*, *Mekh. Tverd. Tela*, 2006, no. 6.
16. Nikitin, L.V. and Tyurekhodgaev, A.N., Wave Propagation and Vibration of Elastic Rods with Interfacial Frictional Slip, *Wave Motion,* 1990, vol. 12, no. 6.
17. Tyurekhodgaev, A.N. and Sergaziev, M.Zh., Excitation of Resonance Oscillations in a System with Contact Dry Friction, *Proc. Int. Congr. Mechanics and Tribology of Transportation Systems-2003*, vol. 2, Rostov-on-Don: RGUPS, 2003.
18. Tyurekhodgaev, A.N. and Sergaziev, M.Zh., Non-Linear Stabilized Oscilaltions of a Cyclic-Loaded Mechanical System with Dry Friction, *Proc. Int. Congr. Mechanics and Tribology of Transportation Systems-2003*, vol. 2, Rostov-on-Don: RGUPS, 2003.
19. Sultanov, K.S., Numerical Solution to the Problem of Wave Propagation in a Viscous-Elastic Rod with External Friction, *Izv. AN SSSR*, *Mekh. Tverd. Tela*, 1991, no. 6.
20. Smirnov, A.L., Computation of the Process of Impact Submersion of a Pile in Ground. Part I, Mathematical Modeling, *Soviet Mining Science*, 1989, vol. 25, no. 4. указать страницы
21. Smirnov, A.L., Dynamics of Integrated Structures in a Medium under Non-Stationary Pulsed Deformation in Elastic Constructions, *Cand. Sci. (Phys.-Math.) Dissertation*, Novosibirsk, 1990.
22. Stepanenko, M.V., A Method of Analyzing Transient Impulsive Deformation in Elastic Structures, *Soviet Mining Science*, 1976, vol. 12, no. 2, pp. 170-174.
23. Petreev, A.M., and Smolentsev, A.S., Blow Energy Transmission from a Striking Machine Element to a Pipe via Adaptor, *Journal of Mining Science*, 2011, vol. 47, no. 6. 787–797.
24. Isakov, A.L. and Shmelev, V.V., Wave Processes when Driving Metal Pipes into the Ground Using Shock-Pulse Generators, *Journal of Mining Science,* 1998, vol. 34, no. 2, pp. 139–147.